DOI: https://doi.org/10.17816/vto322858

Дифференциальная диагностика очаговых изменений позвоночника с использованием стандартного и радиомического анализа: ретроспективное исследование

Н.И. Сергеев, П.М. Котляров, В.А. Солодкий

Российский научный центр рентгенорадиологии, Москва, Российская Федерация

АННОТАЦИЯ

Обоснование. При обнаружении очаговых изменений в костях врач-рентгенолог должен исключить или подтвердить наличие метастатического характера поражения. Хотя семиотика метастатических и неонкологических изменений по данным магнитно-резонансной томографии (МРТ) достаточно известна, на практике могут встречаться различные сочетания сигнальных характеристик, отражающие течение хронических параллельных процессов, значительно затрудняющих интерпретацию. Использование методов компьютерного анализа изображений имеет большие перспективы и способно повысить диагностическую точность стандартных методов визуализации.

Цель. Повысить точность диагностики рентгенологических заключений очаговых изменений позвоночника с помощью дополнительной оценки изображений алгоритмами компьютерного анализа.

Материалы и методы. Обследованы 30 пациентов, 15 из которых — с метастатическими изменениями в костях вследствие рака молочной железы и ещё 15 — с очаговыми изменениями в костях неонкологической природы. Компьютерный анализ очаговых изменений тел позвонков проведён по T_1ВИ, T_2ВИ, STIR МРТ-последовательностям. Для компьютерного анализа использовали оператор сложности изображения Арцела, гистограммное распределение яркостей.

Результаты. Установлены основные дифференциальные показатели для гемангиомы, условно-нормальных участков костного мозга и метастатических очагов. Оператор сложности изображений Арцела для гемангиомы составил ~0,07, для метастазов (mts) — ~0,05, для позвонка — ~0,04. Гистограммный оператор яркостей для гемангиомы составил ~1,12, для mts — ~0,94. Отличие показателей между собой оказалось равным около 20–25% между гемангиомой и костным мозгом и 35% — между mts и костным мозгом, что позволяет эффективно использовать перечисленные показатели вместе с другими маркёрами.

Заключение. Полученные в работе с помощью радиомического анализа критерии дифференциальной диагностики показали значимые различия между очаговыми изменениями в позвонках различной этиологии. С математической точки зрения они носят рекомендательный характер, а в центре системы принятия решений остаётся врач с его опытом.

Ключевые слова: метастазы в кости; онкология; магнитно-резонансная томография; радиомика.

Как цитировать:
Сергеев Н.И., Котляров П.М., Солодкий В.А. Дифференциальная диагностика очаговых изменений позвоночника с использованием стандартного и радиомического анализа: ретроспективное исследование // Вестник травматологии и ортопедии им. Н.Н. Приорова. 2023. Т. 30, № 1. С. 77–85. DOI: https://doi.org/10.17816/vto322858

Рукопись получена: 12.04.2023 **Рукопись одобрена:** 26.04.2023 **Опубликована:** 07.06.2023

DOI: https://doi.org/10.17816/vto322858

Differential diagnosis of focal changes in the spine using standard and radiomic analysis

Nikolay I. Sergeev, Petr M. Kotlyarov, Vladimir A. Solodky

Russian Scientific Center of Roentgenoradiology, Moscow, Russian Federation

ABSTRACT

BACKGROUND: If focal changes in the bones are detected, the radiologist must exclude or confirm the presence of a metastatic lesion. Although the semiotics of metastatic and non-oncological changes according to magnetic resonance imaging (MRI) data is well known, in practice, there may be various combinations of their characteristics that are influenced by other chronic diseases and parallel processes, which significantly complicate interpretation. The use of computer image analysis methods has great prospects and can improve the diagnostic accuracy of standard imaging methods.

OBJECTIVE: To improve the accuracy of diagnosing radiographic findings of focal changes in the spine using additional image evaluation by computer analysis algorithms.

MATERIALS AND METHODS: Thirty patients were examined, and 15 of them had metastatic bone lesions from breast cancer, and 15 had focal changes in the spine of a non-oncological nature. Computer analysis of focal changes in the vertebral bodies was conducted according to T_1WI, T_2WI, and STIR MRI sequences. For the computer analysis, the operator of the complexity of the image Arzela and histogram distribution of brightness were used.

RESULTS: The main differential indicators for hemangioma, conditionally normal areas of the bone marrow, and metastatic foci have been established. The Arzela data image complexity operator was approximately 0.07 for hemangioma, approximately 0.05 for metastases (mts), and approximately 0.04 for vertebrae. The brightness histogram operator was approximately 1.12 for haemangioma and approximately 0.94 for mts. Regarding the difference between indicators, the difference is 20%–25%, between hemangioma and bone marrow and 35% between mts and bone marrow, which make it possible to effectively use these indicators together with other markers.

CONCLUSION: The criteria for differential diagnosis obtained using radiomic analysis showed significant differences between focal changes in the vertebrae of various etiologies. From a mathematical point of view, they are advisory, and the doctor with experience remains at the center of the decision-making system.

Keywords: bone metastases; oncology; MRI; radiomics.

To cite this article:
Sergeev NI, Kotlyarov PM, Solodky VA. Differential diagnosis of focal changes in the spine using standard and radiomic analysis. *N.N. Priorov Journal of Traumatology and Orthopedics*. 2023;30(1):77–85. DOI: https://doi.org/10.17816/vto322858

Received: 12.04.2023 **Accepted:** 26.04.2023 **Published:** 07.06.2023

BACKGROUND

Bone metastases have been reported to occur in approximately 40% of patients with cancer, with varying incidences depending on the primary tumor type and location [1]. Contemporary medical imaging methods, such as multislice computed tomography, magnetic resonance imaging (MRI), and positron emission tomography, have high diagnostic efficiency. However, the variability in the course of bone metastases determines the advantages and disadvantages inherent in each method [2, 3]. Modern image analysis algorithms aim to improve the interpretation of the obtained research results. Patients' conditions can be described in various ways and with varying degrees of detail based on MRI images using different methods, such as pixel-by-pixel analysis of images for various pathologies and modalities [4, 5]. Here, several methods can be selected, which are mainly reduced to certain statistics, namely, brightness statistics, histograms, and distribution of pixel groups (i.e., texture). Because of such large variability in values, despite attempts to systematize and unify the approach, at this stage, many different methods of analysis often provide contradictory or doubtful results [6]. Gradually, with the improvement in the methods of recognizing an object (disease), an increasing number of signs are included, leading to direct recognition of objects by a person or a neural network [7, 8].

Therefore, this study aimed to improve the accuracy of diagnostic radiographic findings of focal changes in the spine using an additional image evaluation by computer analysis algorithms.

MATERIALS AND METHODS

Study design

This was a single-center retrospective study. A total of 30 patients were included in this study. MRI data of the patients with focal changes in the spine were independently analyzed by two radiologists with >10 years of experience. If the conclusions of the radiologists coincided, the results of the images were divided into three groups (hemangiomas, metastasis, and normal bone marrow), after which they were subjected to radiomic analysis with the identification of features characteristic of each group.

Terms and conditions

MRI images were retrospectively analyzed on the workstation "PO Vidar" (Russia). Images were analyzed using the specialized software "Radiomica Applata" (Germany). MRI examinations were performed using standard protocols approved by the Russian Scientific Center of Roentgenology and Radiology (Moscow).

Methods for assessing target indicators

Research methods

The diagnostic algorithm used MRI from devices from various manufacturers (Aera, Siemens, Germany; Atlas, Canon, Japan) with a magnetic field strength of 1.5 T. All patients with cancer underwent bone scintigraphy within the examination protocol. All studies were independently evaluated by two radiologists with >10 years of experience to increase the significance.

Analysis methods

The key MRI sequence for radiomic analysis was T_2-weighted images, and T_1-weighted images and short tau inversion recovery (STIR) were used as auxiliary ones. After image normalization, a pixel-by-pixel analysis was performed with an assessment of the shape and an analysis of the histograms of the image brightness distribution [9]. When using these algorithms, sufficient homogeneity of the object is considered an important parameter. However, this requirement is strong but not always appropriate for many applications. Thus, as it should be in diagnostics, especially in differential diagnostics, additional information about the object should be included while limiting applicability [10].

On the desktop of "Radiomica Applata" (Germany, a proprietary design of IT researchers), the object under study was isolated in the histogram mode, which displays the frequency of occurrence of brightness graphically in the grayscale and enables setting the upper and lower threshold values. For example, when analyzing a hemangioma, if the corresponding brightness window is taken on the histogram, poorly distinguishable objects of a homogeneous structure can be selected (Fig. 1).

As the next extension of the object description, angiogenesis of breast cancer (BC) metastases was used, which has an additional property, namely, a chaotic pathological growth of the vascular network, compared with normal tissue. This determines the image complexity, where the object appears to be more chaotic, i.e., less complex than another, if the sum of boundaries of the parts of its components is less than that of the other under the same measurement conditions. The sum of the boundaries is calculated by the action of the gradient operator on the image under study, that is, a function of pairs of pixels (Arzela operator).

For shape recognition and the use of other modalities, neural networks with the architecture of a multilayer perceptron were used with an input vector of 100 × 100 [11]. The examples described do not require an analysis of the separability of the set of training images (Fig. 2).

In other cases, a self-learning Kohonen network was used for this purpose. The following groups of main images were taken to train the networks:

- Hemangioma.
- Normal tissue.
- Metastases.

Spondylocystitis and areas of fatty degeneration in the vertebrae or the so-called fat deposits, namely, local focal changes with a high-fat content in the presence of intact bone marrow, were used as additional groups.

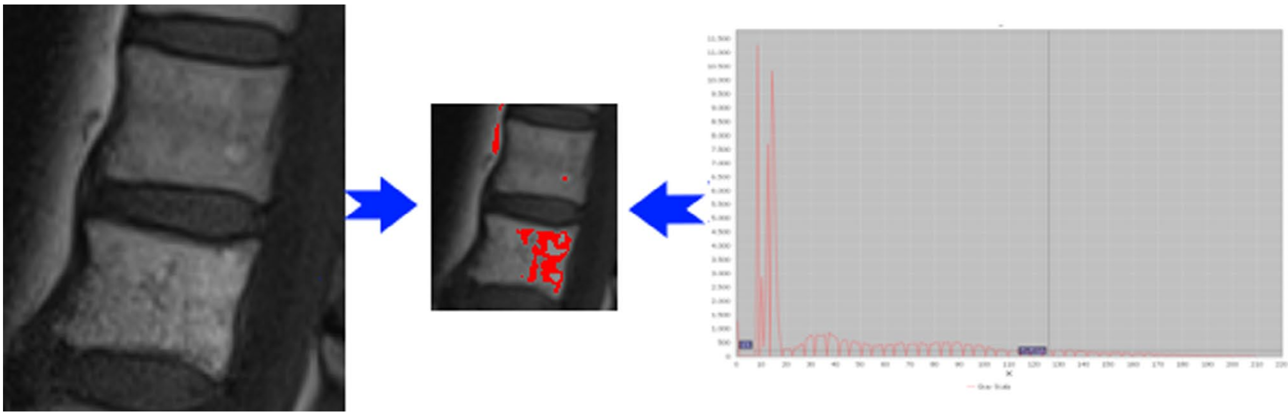

Fig. 1. T_1 tse sag-hemangioma, highlighted with a window on the brightness histogram, which is shown on the right side of the figure.

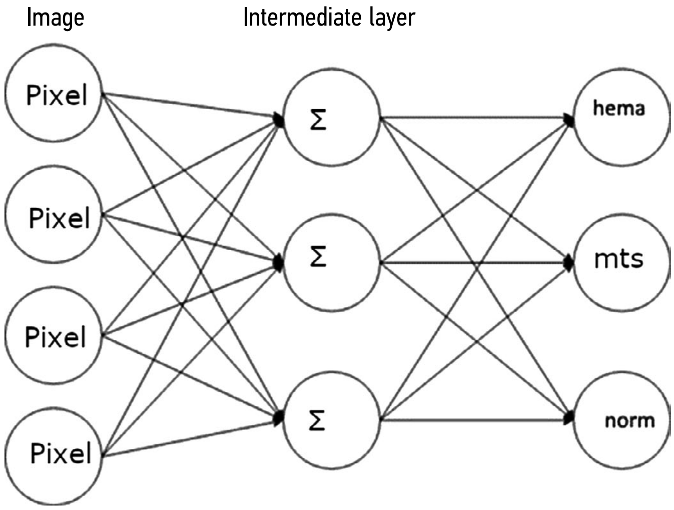

Fig. 2. Multilayer perceptron for recognition in T_2.
Note (here and in Fig. 3). hema — hemangioma, mts — metastasis, norm — normal tissue.

Ethical considerations

Ethical approval was waived due to the retrospective nature of the study.

RESULTS

Participants

The results of the examination of 30 patients with focal changes in the vertebral bodies of the thoracic and lumbar spine were included in this study. Of the 30 patients, 15 had morphologically verified BC with metastatic focal changes in the bones, and 15 did not have a morphologically confirmed diagnosis of a malignant neoplasm, and they were examined due to nonspecific complaints of "pain or discomfort in the spine." The most diagnostically indicative foci were used in the study. In this category of patients, hemangiomas of the vertebral bodies (n=7) and areas of subchondral edema in the vertebral bodies (n=5, 3 of them had spondylodiscitis) were determined. Furthermore, for comparison, areas of local delimited fatty degeneration of the bone marrow were analyzed (n=5), and areas of unchanged vertebrae were measured in five patients. A total of 40 measurements were made in this study.

Primary results

The values of the ratios of light, medium, and dark intensities were obtained when analyzing the intensities in the studied objects. Dark sites were defined as microfoci or the so-called calderas. The ratio of the average brightness of an object (hemangioma, metastasis, or an area of conditionally unaltered bone marrow) to the brightness of the surrounding bone tissue of the vertebral body in grayscale was chosen as a "histogram" assessment. Table 1 shows the radiomic analysis results of hemangiomas. Table 2 shows the analysis of BC metastatic foci with the closest possible clinical characteristics. In the table, microfoci with brightness significantly higher than the average in the region of interest were marked in yellow, those with signal isointense (ISO) to the environment were marked in red, and areas with reduced intensity compared with the average were marked in green.

DOI: https://doi.org/10.17816/VTO322858

Table 1. Results of radiomic analysis of hemangiomas depending on the operators used in T_2WI sag mode

Description of RoI	Arzela RoI	RoI caldera	Arzela data image of the surroundings	RoI/surroundings in gray
Hemangioma-1, T_2-sagittal		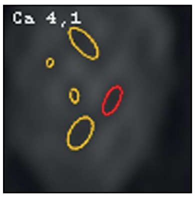		1.27
Hemangioma-1, T_2-sagittal, subtotal		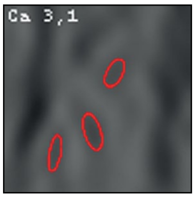		1.16
Hemangioma-2, T_2-sagittal		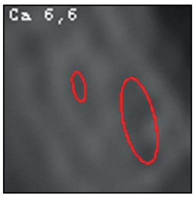	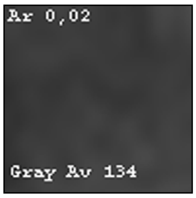	1.16
Hemangioma, T_2-sagittal		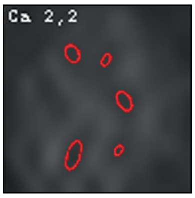		1.11
Fatty degeneration, T_2-sagittal		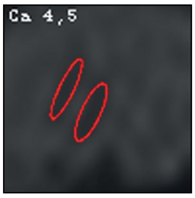		1.07
Hemangioma-2, T_2-sagittal	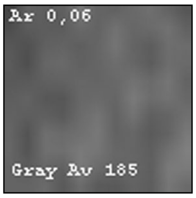	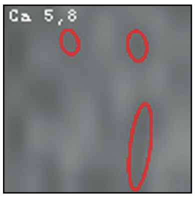		1.17

The hemangioma manifested itself in increased brightness compared with normal tissue, with a ratio of 1.11:1.27 in the cases discussed, increased structuredness (multiple ISO microfoci), and increased complexity (Arzela) to normal tissue. Furthermore, cases of fatty degeneration were reported, the main difference of which, compared with hemangioma, was the environment. Our parameters (intensity statistics, pattern complexity, and the presence of microfoci, which might not be present) did not reflect the environment and imaging mode (e.g., fat suppression) and were thus only necessary but insufficient.

BC metastases appeared to be reduced in brightness compared with normal tissue on a T-weighted image with a ratio of approximately 0.9 (Table 2). Additionally, a certain increase in image complexity was noted. The caldera was distinctly elevated and varied from ISO to darkened, which is expressed as a percentage of the total image area. The study results showed that the main differential indicators of hemangioma, conditionally normal areas of the bone marrow, and metastatic foci were established. The Arzela image complexity operator was approximately 0.07 for hemangiomas, approximately 0.05 for metastases, and approximately 0.04 for vertebrae. The histogram brightness operator was approximately 1.12 for hemangiomas and approximately 0.94 for metastases. The difference between the indicators was about 20%–25% between hemangiomas and bone marrow and 35% between metastases and bone marrow. Therefore, these

Table 2. Results of T_2WI radiomic analysis of breast cancer (РМЖ) metastases

BC metastasis 1		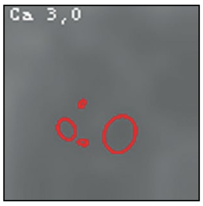		0.915
BC metastasis 2		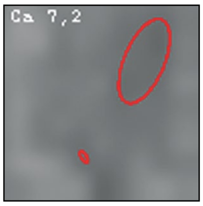	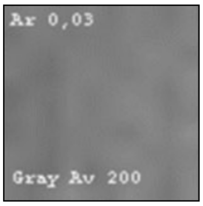	0.965
BC metastasis 3		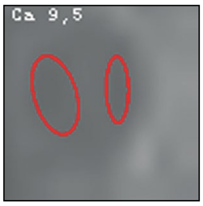	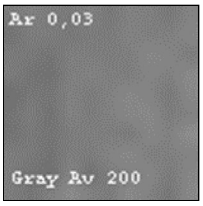	0.945
BC metastasis 4		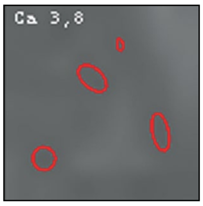	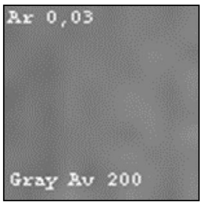	0.88
BC metastasis		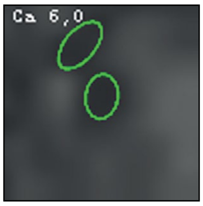		0.98

indicators can be effectively used together with other markers.

Figure 3 shows the result of object recognition from Fig. 1. The Arzela value was superior to that of the "normal" adjacent tissue (leftmost image), which is typical for a hemangioma. Additionally, the ratio of average intensity to "normal" tissue, equal to 1.15, was characteristic of hemangioma. The conditional probabilities of identifying the object were indicated, from which the hemangioma was recognized, with a conditional probability of 0.9 in shape.

Furthermore, as a control measure, the same parameters in the STIR MRI sequence were analyzed, which is considered an important diagnostic component in the differential diagnosis of focal changes in the spine. Here, the hemangioma also manifested itself to be brighter than normal tissue, with a ratio between 1.02 and 1.24 in the cases under consideration. The increased structuredness and increased complexity of the

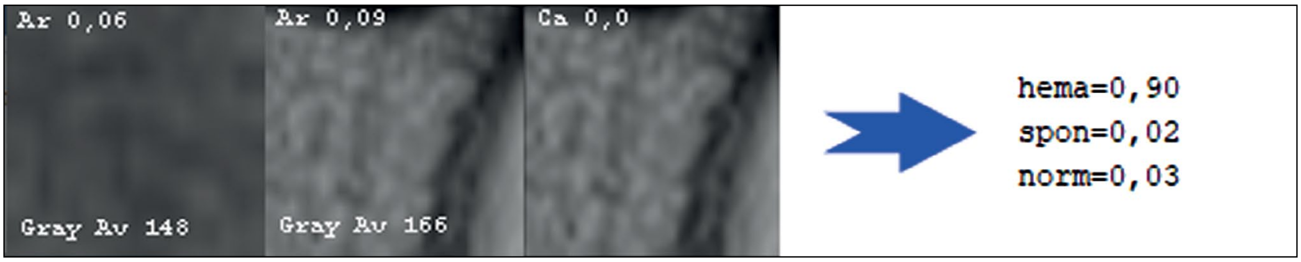

Fig. 3. The results of the analysis of hemangioma by the Artzel drawing complexity operator.

DOI: https://doi.org/10.17816/VTO322858

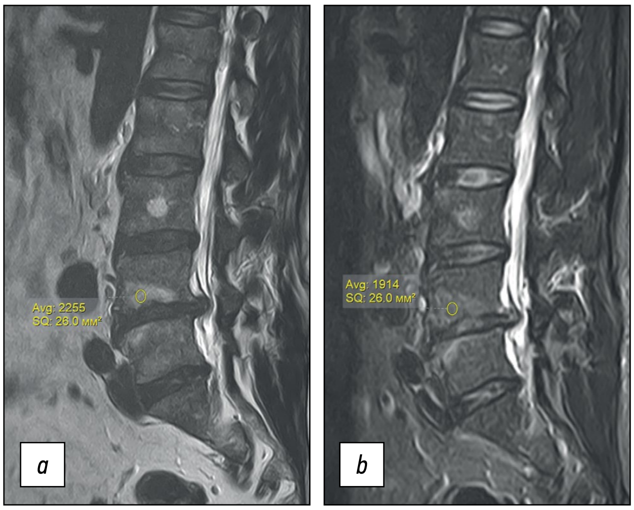

Fig. 4. MRI of the lumbar spine in the sagittal projection. T_2WI, degenerative-dystrophic changes in a patient without an oncological history. *a*) Zones of heterogeneous subcortical edema are determined in the bodies of the vertebrae L_{IV}, L_{V} against the background of a herniated disc. *b*) In the STIR mode, the severity of edema appears to be reduced in relation to T_2WI due to areas of fatty degeneration and subcortical sclerosis.

Arzela operator in relation to normal tissue were important established criteria.

The image analysis operators used did not reveal significant differences in the differential signs of the presented edema and vertebral fat deposit cases. This is probably due to parallel processes, where areas of fatty degeneration with a reduced signal in STIR and uneven zones of subcortical osteosclerosis are determined against the subcortical peritrabecular edema (Fig. 4).

DISCUSSION

Computer analysis methods of images, such as radiomics, texture analysis, and computer aid systems, have great prospects. Some solutions are already being used in practice, such as in screening for focal changes in the lungs, predicting the results of treatment of brain tumors, and direct evaluation of treatment efficiency of BC metastases [12–14]. Although this study demonstrated a rather high efficiency in distinguishing between benign and malignant focal changes in the spine, this can be due to the fact that the clinical cases most typical from a radiographic point of view were analyzed in this study. In practice, several parallel chronic processes pose the greatest difficulty for radiologists in evaluating bones when changes can overlap. Improving the diagnostic efficiency of the method consists of cross-analysis of various sequences and operators and search for new radiomic image markers, which requires further research and a larger number of cases.

Some measurement errors may depend on the difference in image filters implemented on devices from different manufacturers. Thus, more cases and statistical analyses of the results obtained are needed to increase the significance of the results obtained.

CONCLUSION

The differential diagnostic criteria demonstrated in this study, including data obtained using neural networks, are necessary but insufficient from a mathematical point of view and are advisory in nature. Medical specialists with experience are still at the core of the decision-making system.

ДОПОЛНИТЕЛЬНО / ADDITIONAL INFO

Вклад авторов. Все авторы подтверждают соответствие своего авторства международным критериям ICMJE (все авторы внесли существенный вклад в разработку концепции, проведение исследования и подготовку статьи, прочли и одобрили финальную версию перед публикацией).

Author's contribution. Thereby, all authors made a substantial contribution to the conception of the work, acquisition, analysis, interpretation of data for the work, drafting and revising the work, final approval of the version to be published and agree to be accountable for all aspects of the work.

Источник финансирования. Не указан.

Funding source. Not specified.

Конфликт интересов. Авторы декларируют отсутствие явных и потенциальных конфликтов интересов, связанных с публикацией настоящей статьи.

Competing interests. The authors declare that they have no competing interests.

СПИСОК ЛИТЕРАТУРЫ

1. Padalkar P., Tow B. Predictors of survival in surgically treated patients of spinal metastasis // Indian J Orthop. 2011. Vol. 45, N 4. P. 307–313. doi: 10.4103/0019-5413.82333

2. Сергеев Н.И., Фомин Д.К., Котляров П.М., Солодкий В.А. Сравнительное исследование возможностей ОФЭКТ/КТ и магнитно-резонансной томографии всего тела в диагностике костных метастазов // Вестник Российского научного центра рентгенорадиологии. 2015. Т. 15, № 3. С. 8.

3. Haraldsen A., Bluhme H., Røhl L., et al. Single photon emission computed tomography (SPECT) and SPECT/low-dose computerized tomography did not increase sensitivity or specificity compared to planar bone scintigraphy for detection of bone metastases in advanced breast cancer // Clin Physiol Funct Imaging. 2016. Vol. 36, N 1. P. 40–46. doi: 10.1111/cpf.12191

4. Иозефи Д.Я., Сергеев Н.И., Солодкий В.А., Винидченко М.А. Возможности текстурного анализа изображений (коэффициента структурной гетерогенности и карт исчисляемого коэффициента диффузии) в дифференциальной диагностике метастатического поражения костей по данным магнитно-резонансной томографии // Вестник Российского научного центра рентгенорадиологии. 2022. Т. 22, № 3. С. 1–17.

5. Tian Z., Chen C., Fan Y., et al. Glioblastoma and Anaplastic Astrocytoma: Differentiation Using MRI Texture Analysis // Front Oncol. 2019. N 9. P. 876. doi: 10.3389/fonc.2019.00876

6. Литвин А.А., Буркин Д.А., Кропинов А.А., Парамзин Ф.Н. Радиомика и анализ текстур цифровых изображений в онкологии (обзор) // Современные технологии в медицине. 2021. Т. 13, № 2. С. 97–104. doi: 10.17691/stm2021.13.2.11

7. Özgül H.A., Akin I.B., Mutlu U., Balci A. Diagnostic value of machine learning-based computed tomography texture analysis for differentiating multiple myeloma from osteolytic metastatic bone lesions in the peripheral skeleton // Skeletal Radiol. 2023. doi: 10.1007/s00256-023-04333-4. Epub ahead of print.

8. Park H.J., Park B., Lee S.S. Radiomics and Deep Learning: Hepatic Applications // Korean J Radiol. 2020. Vol. 21, N 4. P. 387–401. doi: 10.3348/kjr.2019.0752

9. Shinohara R.T., Sweeney E.M., Goldsmith J., et al. Statistical normalization techniques for magnetic resonance imaging // Neuroimage Clin. 2014. N 6. P. 9–19. doi: 10.1016/j.nicl.2014.08.008

10. Pencheva T.D. Hochaufgelöste MRT zur Quantifizierung veränderter trabekulärer Knochen-Architektur bei Patientinnen mit und ohne Mammakarzinom und osteoporotischer Wirbelkörper-Fraktur: dissertation. München: Universitätsbibliothek der TU München, 2013. Available from: https://mediatum.ub.tum.de/doc/1129206/1129206.pdf. Accessed: 14.05.2023.

11. Steinhauer V., Steinhauer L. Neuroph and DL4J // Java Magazine. 2021. N 6. P. 79–82.

12. Морозов С.П., Кокина Д.Ю., Павлов Н.А., и др. Клинические аспекты применения искусственного интеллекта для интерпретации рентгенограмм органов грудной клетки // Туберкулез и болезни легких. 2021. Т. 99, № 4. С. 58–64. doi: 10.21292/2075-1230-2021-99-4-58-64

13. Ye J., Huang H., Jiang W., et al. Tumor Grade and Overall Survival Prediction of Gliomas Using Radiomics // Scientific Programming. 2021. Vol. 2021. Article ID 9913466. doi: 10.1155/2021/9913466

14. Штайнгауэр В., Сергеев Н.И. Радиомика при раке молочной железы: использование глубокого машинного анализа МРТ-изображений метастатического поражения позвоночника // Современные технологии в медицине. 2022. Т. 14, № 2. С. 16. doi: 10.17691/stm2022.14.2.02

REFERENCES

1. Padalkar P, Tow B. Predictors of survival in surgically treated patients of spinal metastasis. *Indian J Orthop*. 2011;45(4):307–313. doi: 10.4103/0019-5413.82333

2. Sergeev NI, Fomin DK, Kotlyarov PM, Solodkiy VA. Comparative study of the possibilities of SPECT/CT and whole body MRI in the diagnosis of bone metastases. *Vestnik of the Russian Scientific Center of Roentgenoradiology*. 2015;15(3):8. (In Russ).

3. Haraldsen A, Bluhme H, Røhl L, et al. Single photon emission computed tomography (SPECT) and SPECT/low-dose computerized tomography did not increase sensitivity or specificity compared to planar bone scintigraphy for detection of bone metastases in advanced breast cancer. *Clin Physiol Funct Imaging*. 2016;36(1):40–46. doi: 10.1111/cpf.12191

4. Iosefi DYa, Sergeev N, Solodkiy VA, Vinidchenko MA. Possibilities of textural analysis of images (structural heterogeneity coefficient and maps of the apparent diffusion coefficient) for differential diagnosis of metastatic bone lesions according to magnetic resonance imaging. *Vestnik of the Russian Scientific Center of Roentgenoradiology*. 2022;22(3):1–17. (In Russ).

5. Tian Z, Chen C, Fan Y, et al. Glioblastoma and Anaplastic Astrocytoma: Differentiation Using MRI Texture Analysis. *Front Oncol*. 2019;9:876. doi: 10.3389/fonc.2019.00876

6. Litvin AA, Burkin DA, Kropinov AA, Paramzin FN. Radiomics and Digital Image Texture Analysis in Oncology (Review). *Sovrem Tekhnologii Med*. 2021;13(2):97–104. (In Russ). doi: 10.17691/stm2021.13.2.11

7. Özgül HA, Akin IB, Mutlu U, Balci A. Diagnostic value of machine learning-based computed tomography texture analysis for differentiating multiple myeloma from osteolytic metastatic bone lesions in the peripheral skeleton. *Skeletal Radiol*. 2023. doi: 10.1007/s00256-023-04333-4. Epub ahead of print.

8. Park HJ, Park B, Lee SS. Radiomics and Deep Learning: Hepatic Applications; *Korean J Radiol*. 2020;21(4):387–401. doi: 10.3348/kjr.2019.0752

9. Shinohara RT, Sweeney EM, Goldsmith J, et al. Statistical normalization techniques for magnetic resonance imaging. *Neuroimage Clin*. 2014;6:9–19. doi: 10.1016/j.nicl.2014.08.008

10. Pencheva TD. *Hochaufgelöste MRT zur Quantifizierung veränderter trabekulärer Knochen-Architektur bei Patientinnen mit und ohne Mammakarzinom und osteoporotischer Wirbelkörper-Fraktur* [dissertation]. München: Universitätsbibliothek der TU München, 2013. Available from: https://mediatum.ub.tum.de/doc/1129206/1129206.pdf. Accessed: 14.05.2023. (In German).

11. Steinhauer V, Steinhauer L. Neuroph and DL4J. *Java Magazine*. 2021;6:79–82.

12. Morozov SP, Kokina DYu, Pavlov NA, et al. Clinical aspects of using artificial intelligence for the interpretation of chest X-rays. *Tuberculosis and Lung Diseases*. 2021;99(4):58–64. (In Russ). doi: 10.21292/2075-1230-2021-99-4-58-64

13. Ye J, Huang H, Jiang W, et al. Tumor Grade and Overall Survival Prediction of Gliomas Using Radiomics. *Scientific Programming*. 2021;2021:9913466. doi: 10.1155/2021/9913466

14. Steinhauer V, Sergeev NI. Radiomics in Breast Cancer: In-Depth Machine Analysis of MR Images of Metastatic Spine Lesion. *Sovrem Tekhnologii Med*. 2022;14(2):16. doi: 10.17691/stm2022.14.2.02

ОБ АВТОРАХ

*** Сергеев Николай Иванович,** д.м.н.,
ведущий научный сотрудник;
адрес: Россия, 117485, Москва, ул. Профсоюзная, д. 86;
ORCID: 0000-0003-4147-1928;
eLibrary SPIN: 2408-6502;
e-mail: sergeevnickolay@yandex.ru

Котляров Петр Михайлович, д.м.н., профессор;
ORCID: 0000-0003-1940-9175;
eLibrary SPIN: 1781-2199;
e-mail: marnad@list.ru

Солодкий Владимир Алексеевич, д.м.н., профессор,
академик РАН;
ORCID: 0000-0002-1641-6452;
eLibrary SPIN: 9556-6556;
e-mail: director@rncrr.ru

* Автор, ответственный за переписку / Corresponding author

AUTHORS INFO

*** Nikolai I. Sergeev,** MD, Dr. Sci. (Med.),
leading researcher,
address: 86 Profsoyuznaya Str., 117485, Moscow, Russia;
ORCID: 0000-0003-4147-1928;
eLibrary SPIN: 2408-6502;
e-mail: sergeevnickolay@yandex.ru

Petr M. Kotlyarov, MD, Dr. Sci. (Med.), Professor;
ORCID: 0000-0003-1940-9175;
eLibrary SPIN: 1781-2199;
e-mail: marnad@list.ru

Vladimir A. Solodkiy, MD, Dr. Sci. (Med.), Professor,
Academician of RAS;
ORCID: 0000-0002-1641-6452;
eLibrary SPIN: 9556-6556;
e-mail: director@rncrr.ru